Supporting Information
Adsorption Energy Scaling Relation on Bimetallic Magnetic Surfaces: Role of Surface Magnetic Moments

Swetarekha Ram, Seung-Cheol Lee* and Satadeep Bhattacharjee*

Indo-Korea Science and Technology Center (IKST), Bangalore 560065, India

E-mail:seungcheol.lee@ikst.res.in, satadeep.bhattacharjee@ikst.res.in

June 16, 2020

1 Details of bulk TM compounds

We have used $L1_0$ phase of bulk NiPt, FePt, FePd, MnPt, MnPd, CoPt and $L1_2$ phase of $CoPt_3$, $MnPt_3$, $FePt_3$, $NiPt_3$ and Co_3Pt for calculating theoretical lattice parameter. The obtained optimized lattice parameters along with the available experimental and other theoretical values are reported in Table S1. We have constructed (111) surface from the optimized lattice parameters to calculate the adsorption energy of adatoms.

2 Adsorption energy of magnetic bimetallic transition metal surfaces

The calculated adsorption energy for O and OH molecule in bimetallic magnetic transition metal (TM) surface and the monometallic TM surface in close-packed structure is presented in Table S2.

2.1 Parameters associated with scaling relation

Pearson correlation coefficient matrices are calculated for the bimetallic magnetic TM surfaces, which is a measure of the linear association between two variables x and y, where $x, y \in \{\omega_i\}$. The parameters of the set $\{\omega_i\}$ is presented in Table S3.

3 DDEC6 charges of O and OH adatoms

We have reported the values calculated from DDEC6 analysis in Table S5. For any electronic charge partitioning scheme, the absolute magnitude of the charges in the particular system is of less importance than their relative charges.

Table S1 The theoretical lattice parameters for bimetallic TM magnetic compounds in bulk form along with available experimental (in parentheses) and other theoretical values and the calculated magnetic moment for bimetallic TM magnetic compounds with other available theoretical and experimental data (in parentheses).

Compounds	a in Å	c in Å	Mag. mom in μ_B
MnPd	4.11, (3.82^b)	3.58, (3.68^b)	3.42, 3.78^n, (4.4^n)
MnPt	4.09, (4.0^c) 3.89^f	3.62, (3.67^c) 3.64^f	3.59, 4.17^i
FePd	3.84, (3.85^c)	3.77, (3.71^c)	3.25, (3.2^o)
FePt	3.87, (3.852^a) 3.838^a, 3.88^f	3.75, (3.713^a), 3.739^a, 3.78^f	3.32, 2.93(Fe),0.29(Pt)^p
Co$_3$Pt	3.67, 3.66^d	-	5.75, 5.66^l
MnPt$_3$	3.94, 3.91^e 3.93^e	-	4.2, 4.08^l, (4.04^m)
FePt$_3$	3.92, (3.866^a) 3.88^g, 3.91^a	-	4.39, 3.30^i, 4.454^l
CoPt	3.82, 3.79^f	3.70^f	2.33, 1.6(Co)^k,0.3(Pt)^k
CoPt$_3$	3.89, 3.83^d	-	3.27, 2.29^i (2.43^j), 2.652^l
NiPt	3.85, 3.81^d	3.63, 3.53^d	2.15, 1.035 ^{i}
NiPt$_3$	3.89, 3.89^h	-	0.81

a[1], b[2], c[3], d[4], e[5], f[6], g[7], h[8], i[9], j[10], k[11], l[12], m[13], n[14], o[15], p[16]

2

Table S2 Adsorption energy, ΔE_{ads} for stable site (fcc site) of bimetallic TM magnetic systems and monometallic TM (Top-ste) in close packed surface, for *O and *OH adsorbate.

Systems	ΔE_{ads} (eV)		Systems	ΔE_{ads} (eV)	
	*O	*OH		*O	*OH
MnPd	-6.18	-3.98	Fe	-7.02	-3.83
MnPt	-6	-3.66	Pd	-4.6	-2.17
FePd	-6.05	-3.75	Pt	-4.53	-2.03
FePt	-5.79	-3.47	Co	-4.49	-2.66
Co$_3$Pt	-5.89	-3.56	Ni	-3.43	-1.94
MnPt$_3$	-5.1	-2.89	Au	-3.33	-1.49
FePt$_3$	-5.01	-2.8	Ag	-3.73	-2.16
CoPt	-5.37	-3.14	Cu	-3.2	-2.23
CoPt$_3$	-4.96	-2.69			
NiPt	-4.84	-2.5			
NiPt$_3$	-4.84	-2.57			

Table S3 Average valence electron (NV_{av}), work function (ϕ), of clean slab as well as with the presence of adsorbates, magnetic moment projected on surface, m_{surf}, net charge transfer δ^- with the presence of O and OH molecule and the adsorption energy of O and OH adsorbate in magnetic bimetallic TM surface.

Systems	NV_{av}	ϕ_{slab}	m_{surf}	ΔE^O_{ads}	δ^-_O	ϕ_O	ΔE^{OH}_{ads}	δ^-_{OH}	ϕ_{OH}
MnPd	8.5	4.47	2.05	-6.18	-0.36	5.37	-3.98	-0.2	4.17
MnPt	8.5	4.72	1.97	-6	-0.32	5.29	-3.66	-0.19	4.55
FePd	9	4.72	1.7	-6.05	-0.36	5.42	-3.75	-0.17	3.26
FePt	9	4.85	1.73	-5.79	-0.34	5.48	-3.47	-0.16	3.43
Co$_3$Pt	9.25	5.03	1.52	-5.89	-0.33	5.54	-3.56	-0.15	3.26
MnPt$_3$	9.25	5.24	1.03	-5.1	-0.29	5.68	-2.89	-0.17	3.73
FePt$_3$	9.5	5.38	1.08	-5.01	-0.3	5.75	-2.8	-0.17	3.674
CoPt	9.5	5.11	1.20	-5.37	-0.31	5.69	-3.14	-0.14	3.52
CoPt$_3$	9.75	5.33	0.74	-4.96	-0.27	5.78	-2.69	-0.13	3.65
NiPt	10	5.33	0.54	-4.84	-0.25	5.75	-2.5	-0.15	3.62
NiPt$_3$	10	5.51	0.29	-4.84	-0.25	5.86	-2.57	-0.11	3.69

Table S4 Correlation between selected variables, $\{\omega_i\}$ and the adsorption energy of O and OH adsorbate. The slope and the intercept of adsorption energies as a function of work function of slab (ϕ_{slab}), average valence electron (NV_{av}) for bimetallic magnetic TM surfaces with O and OH adsorption. All parameters are linearly correlated with adsorption energy.

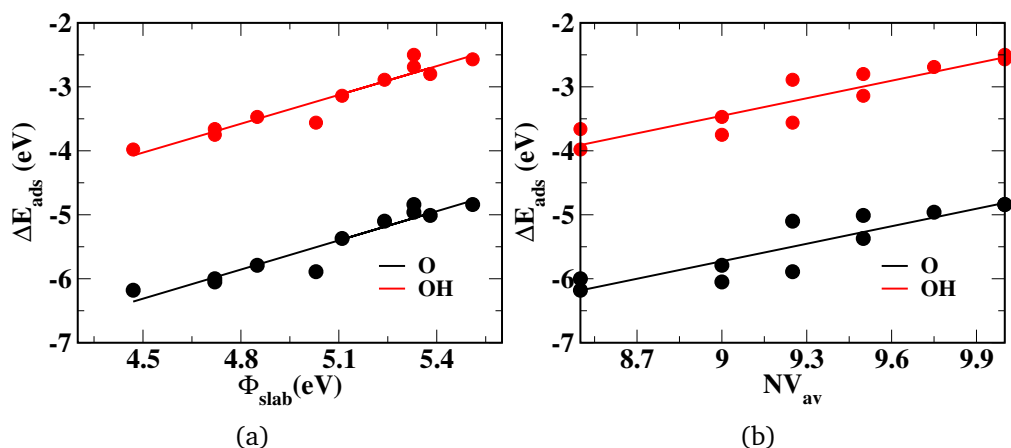| Plots	O		OH	
	slope	intercept	slope	intercept
ϕ_{slab} vs ΔE_{ads}	1.52	-13.15	1.5	-10.79
NV_{av} vs ΔE_{ads}	0.91	-13.94	0.8	11.68

(a)　　　　　　　(b)

Figure S1 Adsorption energies as a function of (a) work function of slab (ϕ_{slab}), (b) the average valence electron (NV_{av}) of bimetallic magnetic TM surface. The adsorption energy scale linearly with all parameters in both O and OH adsobate.
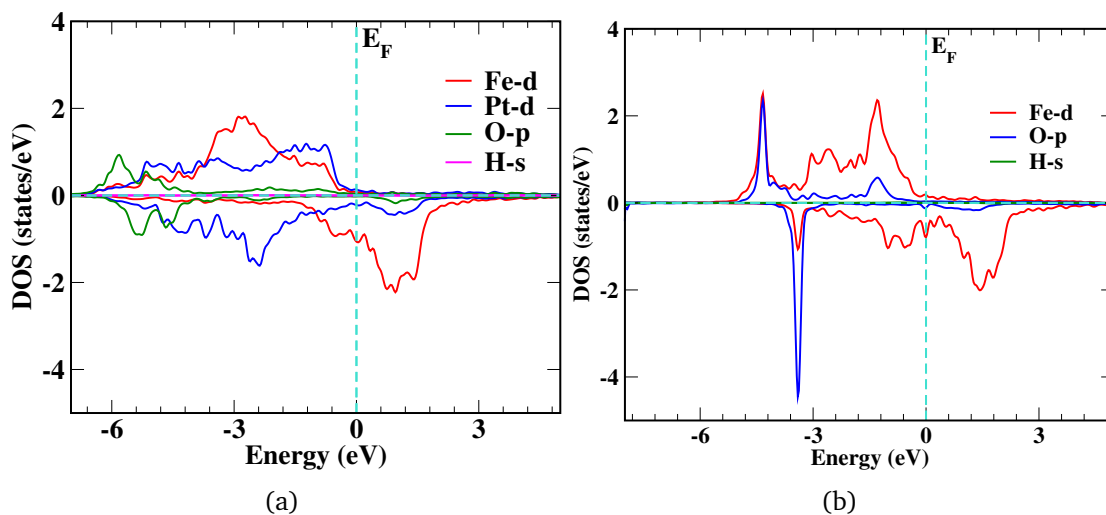

(a)　　　　　　　(b)

Figure S2 DOS for (a) FePt with *OH adsorption, (b) for Fe with *OH adsorption. The hybridization of Fe-d with Pt-d states is significant in majority spin only for FePt, whereas charge transfer occurs from Fe to Pt in the minority spin of FePt. It is the majority spin d-states which strongly hybridized with p-states of O-atoms in FePt. The scenario is almost similar with the O adsorption. The DOS profile remains almost similar as FePt for other bimetallic magnetic TM surface and for monometallic TM, it is similar with Fe.
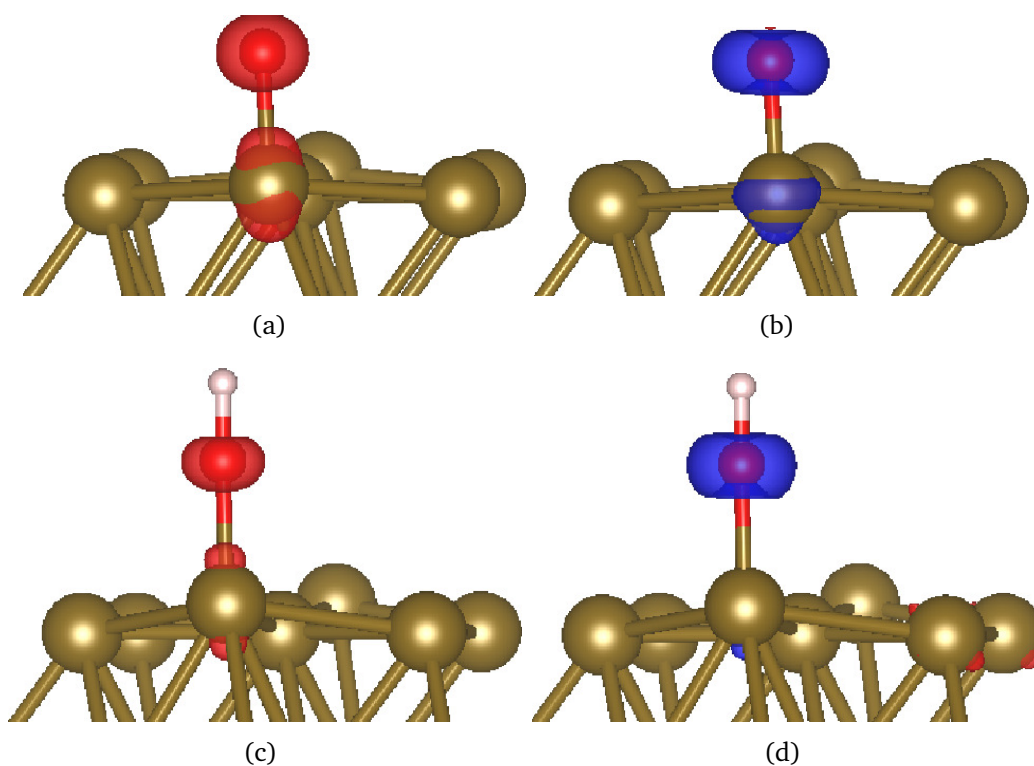
(a)   (b)

(c)   (d)

Figure S3 Iso-surface of differential charge density for (a, c) majority spin of Fe with *O and *OH adsorption, respectively (b, d) minority spin of Fe with *O and *OH adsorption, respectively. The red and blue colors represent the electron accumulation and depletion, respectively. Charge density isosurface was set to 0.005 e^{-3}. The sphere in golden, red and white color represents Fe, O, H atoms respectively. The accumulated charge in *O is more abundant than that in *OH, suggesting that the chemical bond for the *O adsorption is more stable than that for *OH adsorption. A similar observation is also noticed for remaining materials under study.

Table S5 Adsorption energy ΔE_{ads}, net DDEC6 charges of O and OH adatom in *O and *OH adsorption.

Systems	ΔE_{ads} (eV)		DDEC6	
	*O	*OH	δ_O^-:O	δ_{OH}^-:OH
MnPd	-6.18	-3.98	-0.36	-0.2
MnPt	-6	-3.66	-0.32	-0.19
FePd	-6.05	-3.75	-0.36	-0.17
FePt	-5.79	-3.47	-0.34	-0.16
Co$_3$Pt	-5.89	-3.56	-0.36	-0.15
MnPt$_3$	-5.1	-2.89	-0.29	-0.17
FePt$_3$	-5.01	-2.8	-0.3	-0.17
CoPt	-5.37	-3.14	-0.31	-0.14
CoPt$_3$	-4.96	-2.69	-0.27	-0.13
NiPt	-4.84	-2.5	-0.25	-0.15
NiPt$_3$	-4.84	-2.57	-0.25	-0.11
Fe	-7.02	-3.83	-0.32	-0.24
Pd	-4.6	-2.17	-0.36	-0.34
Pt	-4.53	-2.03	-0.29	-0.29
Co	-4.49	-2.66	-0.3	-0.26
Ni	-3.43	-1.94	-0.3	-0.3
Au	-3.33	-1.49	-0.37	-0.37
Ag	-3.73	-2.16	-0.47	-0.43
Cu	-3.2	-2.23	-0.42	-0.37

Table S6 Adsorption energy, ΔE_{ads} for stable site of bimetallic TM magnetic systems for *CH$_x$ and *NH$_x$ adsorbate, where x= 1,2.

Systems	ΔE_{ads} (eV)					
	*C	*CH	*CH$_2$	*N	*NH	*NH$_2$
MnPd	-6.53	-6.07	-4.16	-5.53	-4.71	-3.26
MnPt	-6.51	-6.11	-4.11	-5.4	-4.72	-2.46
FePd	-6.64	-6.14	-4.07	-5.26	-4.66	-2.78
FePt	-6.24	-6.25	-4.16	-5.16	-4.55	-2.72
Co$_3$Pt	-6.73	-6.23	-4.1	-5.34	-4.65	-2.82
MnPt$_3$	-6.44	-6.09	-4.24	-4.78	-4.23	-2.57
FePt$_3$	-6.54	-6.2	-4.2	-4.68	-4.16	-2.47
CoPt	-6.7	-6.2	-4.1	-5.01	-4.37	-2.63
CoPt$_3$	-6.8	-6.34	-3.78	-4.84	-4.2	-2.56
NiPt	-6.84	-6.23	-4.15	-4.95	-4.14	-2.56
NiPt$_3$	-6.88	-6.43	-4.22	-4.85	-4.21	-2.57

References

[1] M. Sternik, S. Couet, J. Łażewski, P. Jochym, K. Parlinski, A. Vantomme, K. Temst and P. Piekarz, *Journal of Alloys and Compounds*, 2015, **651**, 528–536.

[2] T. Hori, Y. Tsuchiya, Y. Ishii and K. Hojou, *Materials transactions*, 2002, **43**, 436–438.

[3] P. Villars, L. Calvert and W. Pearson, *American Society for Metals, 1985,*, 1985, 3258.

[4] o. Pearson, WB, *Vols. I and II (Pergamon Press, Oxford, 1964, 1967)*, 1958.

[5] S. C. Hong, *Journal of the Korean Physical Society*, 2008, **53**, 1525–1528.

[6] A. Dannenberg, M. E. Gruner, A. Hucht and P. Entel, *Physical review B*, 2009, **80**, 245438.

[7] N. Tobita, N. Nakajima, N. Ishimatsu, H. Maruyama, K. Shimada, H. Namatame and M. Taniguchi, *Journal of the Physical Society of Japan*, 2010, **79**, 024703.

[8] A. Pisanty, C. Amador, Y. Ruiz and M. de la Vega, *Zeitschrift für Physik B Condensed Matter*, 1990, **80**, 237–239.

[9] A. Dannenberg, M. E. Gruner and P. Entel, Journal of Physics: Conference Series, 2010, p. 072021.

[10] F. Menzinger and A. Paoletti, *Physical Review*, 1966, **143**, 365.

[11] P. He, W. A. McGahan, J. A. Woollam, F. Sequeda, T. McDaniel and H. Do, *Journal of applied physics*, 1991, **69**, 4021–4028.

[12] M. Kumar, T. Nautiyal and S. Auluck, *Journal of alloys and compounds*, 2009, **486**, 60–65.

[13] B. Antonini, F. Lucari, F. Menzinger and A. Paoletti, *Physical review*, 1969, **187**, 611.

[14] W. Jun-Fei, C. Wen-Zhou, J. Zhen-Yi, Z. Xiao-Dong and S. Liang, *Chinese Physics B*, 2012, **21**, 077102.

[15] V. Moruzzi and P. Marcus, *Physical Review B*, 1993, **48**, 16106.

[16] J. Staunton, S. Ostanin, S. Razee, B. Gyorffy, L. Szunyogh, B. Ginatempo and E. Bruno, *Physical review letters*, 2004, **93**, 257204.